

# Competitive adsorption of phosphate and carboxylate with natural organic matter on hydrous iron oxides as investigated by chemical force microscopy

David I. Kreller, Graham Gibson, William Novak, Gary W. Van Loon,  
J. Hugh Horton\*

*Department of Chemistry, Queen's University, Kingston, ON, Canada K7L 3N6*

Received 28 March 2002; accepted 27 June 2002

## Abstract

The behaviour of phosphate and natural organic matter (NOM) in soils and aqueous media is strongly influenced by their association with surfaces of colloidal mineral oxide and oxyhydroxide particles of iron. Here we investigate the interaction of atomic force microscope (AFM) tips terminated with bis(11-thioundecanoic)phosphate and 16-thiohexadecanoic acid as a function of pH in the context of competitive phosphate–organic matter adsorption interactions at the surface of hydrous iron oxide colloids. Experiments were carried out on unmodified colloids as well as colloids coated with gallic acid, tannic acid or peat-derived humic material. The colloids were also examined by infrared spectroscopy (IR) and zeta potentiometry. Force titrations on a gallic acid control surface revealed that the main mode of interaction of this compound with the tips was hydrogen bonding. A strong interaction in the pH range 4–8 observed for the PO<sub>2</sub>H probe on the unmodified iron (hydroxy)oxide was attributed to a specific adsorption reaction with an A-type Fe–OH surface site. The CO<sub>2</sub>H tip displayed a strong but less specific interaction that extended over the pH range 4–10. Force titrations of probes against colloids post-precipitated with gallic acid, tannic acid or peat-derived humic material were significantly different than for the unmodified surfaces. Surface-bound organic molecules reduced the specific mid pH range interactions and gave rise to two new force titration features with maxima about pH 4 and 8, which were assigned to H-bonding between the probes and benzoic and phenolic groups of surface-bound organic acids, respectively.

© 2002 Elsevier Science B.V. All rights reserved.

*Keywords:* Phosphate; Iron oxide; Colloid; Atomic force microscopy; Tannic acid

## 1. Introduction

The adsorption of phosphates and organic compounds from solution onto surfaces of hydrous iron and aluminum oxides has been studied extensively. It is known that these compounds

\* Corresponding author. Tel.: +1-613-533-2379; fax: +1-613-533-6669

E-mail address: [hortonj@chem.queensu.ca](mailto:hortonj@chem.queensu.ca) (J.H. Horton).

along with other species adsorb at these mineral surfaces in the natural environment, affecting their bio-availability and relative mobility [1]. In fact, it is believed that the distribution of these species in a range of environmental systems is dominated by their surface-adsorbed forms, and that their adsorption underlies the main mechanisms for their sedimentation and movement. Both phosphate and organic compounds are known to interact with similar surface sites on hydrous metal oxide particle surfaces, and their competitive binding interactions have important consequences with regard to agricultural and forest soils, fresh water and marine ecosystems, and chemical water and wastewater treatment [2].

The adsorption interactions of phosphate and organic species at mineral surfaces are complex, and a variety of analytical methods have been employed for their investigation. The most widely used are solution techniques, in which removal of a species from solution by adsorption is monitored by determining the concentration of the species under investigation prior to and after equilibrium with suspended solids has been reached. Solution studies of the competitive adsorption of phosphate with organic compounds including malic and oxalic acid in tropical soils [3], sulphate and oxalic acid on goethite [4], and with inorganic ions on goethite in marine electrolytes [5] have been reported. Infrared spectroscopy (IR) has been employed extensively to study phosphate adsorption on goethite [6], and has provided important insight into the identity of active surface sites involved in phosphate adsorption as well as the structures of adsorbed species. A detailed IR investigation of the adsorption of benzoic and phenolic compounds on goethite has been reported [7]. Zeta potentiometry is frequently used to obtain surface potential information, and has recently been used to investigate effect of mono- and multilayer phosphate adsorption on the surface charge of goethite [8–10]. Modern ultra high vacuum surface analytical methods including X-ray photoelectron spectroscopy and thermally programmed desorption have also been used to examine phosphate adsorbed on an iron oxide single crystal surface [11]. These latter experiments are somewhat less relevant than the solution-based

experiments since the samples have been removed from solution, dried and placed under high vacuum.

Scanning probe microscopic methods permit topographical imaging and the investigation of chemical interactions at the surfaces of non-conducting substrates, making them useful for studying a number of environmentally relevant surface interactions [12]. Experiments may be carried out in solution, allowing real systems to be studied. We have recently reported [13] on the use of chemical force microscopy (CFM) as a method to probe the interaction between solution phase species, in particular orthophosphate species, and hydrous iron oxide colloids. In order to demonstrate the applicability of this method to the study of colloidal systems, our previous work used a phosphate-terminated atomic force microscope (AFM) tip to probe a series of well-characterised colloids, by means of (chemical) force titrations. In this method the adhesive interaction between tip and sample is measured as a function of pH. Care is required in interpreting results of such titrations as the interaction between the tip and sample in CFM may differ significantly from that of a solution phase species; in particular, the ionization constants of acidic or basic functional groups that terminate self-assembled monolayers often differ from those of the corresponding solution phase species. Force titration curves were performed first on a test system consisting of a bis(11-thioundecyl)phosphate tip on an annealed Au surface coated with a SAM of the same substance. The curve obtained was similar in profile to those obtained using carboxylate and diprotic phosphate tips by other workers. A force titration profile of an unmodified hydrous iron oxide colloid was also carried out. The effect of post-precipitating (i.e. reacting the pre-formed colloidal particles with some solution phase species to deposit a surface layer of that species) the colloid with orthophosphate was to modify the force titration profile considerably, resulting in one that indicated adsorption of the phosphate from solution in a bidentate fashion on the surface. This is consistent with previous IR work on these colloids. Colloids postprecipitated with dimethyl phosphate demonstrated similar

bidentate adsorption of the phosphate. However, in this case non-polar and non-ionizable methyl groups were exposed on the surface, leading, as might be expected, to adhesive interactions that were independent of pH.

In the present study, we examine in greater detail the adsorption interactions between the surfaces of hydrous iron oxide particles and AFM probes terminated with carboxylate as well as phosphate functional groups. We also investigate the effects that various types of surface-adsorbed organic matter have on the affinity of the iron colloids towards the functional groups on the probe. To this end, using phosphate and carboxylate tips (terminated with bis(11-thioundecyl)phosphate and 16-thiohexadecanoic acid, respectively), we have conducted force titrations of unmodified hydrous iron oxide colloids as well as colloids coated with gallic acid (3,4,5-trihydroxybenzoic acid), tannic acid and a water-soluble fraction derived from peat. The soluble portion of peat is considered to be a source of impure humic material, which is an ubiquitous component of the organic fraction of soil and of natural organic matter (NOM) in water. The colloids were characterized by standard AFM imaging. IR spectroscopy and zeta potentiometry were also used to determine the effects of the adsorbed species on the structural properties and surface charge of the colloids.

CFM results for hydrous iron oxide particles post-precipitated with gallic acid are compared to control samples of gallic acid deposited directly on a mica support. Gallic acid was chosen because it is a small organic acid whose adsorption properties have been well-characterised [7] as well as the fact that it is a subunit of the more chemically complex tannic acid molecule. Tannic acid consists of a glucose centre to which a variable number of gallic acid and benzoic acid end-groups are attached through ester linkages [14]. Tannic acid and reference humic material in turn may be considered to be sequentially more complex model compounds for NOM found in soils, groundwater and wastewater. Finally, the effect of the further complexation of surface-adsorbed tannic acid with Fe(III) ions on the interaction with the  $-\text{PO}_2\text{H}$  probe was

investigated, to study bridging organic matter– $\text{Fe}^{3+}$ –phosphate interactions, which are known to be important in the chemistry of Podzolic soils.

We show that chemical force titrations can be a useful method for examining the pH dependence of the adsorption interactions of phosphate and carboxylate species with colloidal particles of hydrous iron oxide. We find that the CFM experiments give insight into how organic species adsorbed from solution impact the surface properties of the hydrous iron oxide particles to which they are bound, and give rise to competitive adsorption interactions with phosphate and other ions in solution.

## 2. Experimental

IR spectra were acquired using a Nicolet Avatar 360 E.S.P. FT-IR Spectrometer (Madison, Wisconsin, USA) with a single reflection diamond ATR accessory.

All AFM image data shown were acquired using a PicoSPM operated in MAC mode (Molecular Imaging, Tempe, Arizona), using a Nanoscope IIE controller (Digital Instruments, Santa Barbara, CA). Images were acquired under ambient conditions, as well as under solutions of various pH. The MAC mode is essentially the same as tapping mode, except that the cantilever is magnetically coated and is driven by an external oscillating magnetic field [15]. The cantilevers had a resonance frequency of  $\sim 100$  kHz. All images were acquired under ambient conditions, at the fundamental resonance frequency of the Si cantilevers. The cantilevers used for image acquisition were terminated with standard  $\text{Si}_3\text{N}_4$  tips. Height and phase shift data were all recorded simultaneously, as a function of both cantilever oscillation amplitude ( $A_o$ ) and set point ratio  $r_{\text{sp}} = A_{\text{sp}}/A_o$ . Images were recorded at scan rates of 1.2 Hz using a  $30 \times 30 \mu\text{m}^2$  scanner.

Adhesion data were obtained using the same apparatus. In the force titration experiments, force–distance curves were acquired with the sample immersed under freshly prepared unbuf-

ferred NaOH or HCl solutions of pH ranging from 2 to 12. Unbuffered solutions were chosen in order to avoid potential competitive adsorption of buffer ions in solution on the probe–substrate interactions. Solutions were checked after each experiment to ensure that their pH had not changed significantly. Experiments were carried out at low ionic strength conditions ( $0.01 \text{ mol l}^{-1}$ ), i.e. the only ions in solution were those introduced by pH adjustment with NaOH and HCl. Some 300–500 force–distance curves were obtained for each sample. The reported values of the adhesive interaction are an average of all the force curves obtained while the reported errors reflect the standard deviation of the data.

The AFM tips used in the adhesion force measurements were standard silicon nitride cantilevers (Digital Instruments, Santa Barbara, CA) coated with 200 nm of Au by thermal vapour deposition. The Au-coated tips were functionalised with  $-\text{PO}_2\text{H}$  end groups by immersion in a 1 mM octadecanol solution of bis(11-thioundecyl)phosphate [16] for 48 h.  $-\text{CO}_2\text{H}$  coated tips were similarly prepared by immersion in a 1 mM methanol solution of 16-thiohexadecanoic acid (Aldrich, 95%) for 24 h. The force constants of the cantilevers ranged from 0.2 to  $1.0 \text{ Nm}^{-1}$  as determined by the method of Hutter and Bechhoefer [17]. Variation in tip radii affects the magnitude of CFM forces measured (due to changing tip–sample contact areas) and as expected, adhesive forces seen in repeated experiments on the same experimental probe and substrate combination but using different tips were found to vary by  $\pm 20\%$ . However, despite variation in the absolute magnitude of the tip–sample adhesive forces, the shapes of the titration curves as a function of pH in the various experimental systems were reproducible. It is important to note that a single AFM tip was used in acquiring all the data in each presented pH series, to allow the best comparison of the shapes of various force titration curves.

The iron oxyhydroxide colloids were prepared by hydrolytic precipitation from  $\text{FeCl}_3$  solution and collected for AFM/CFM experiments as outlined in detail elsewhere [13]. Surface adsorption of organic compounds onto the colloids was

achieved by suspending particles aged for 20 min in solutions to which excess amounts of the compound to be surface-adsorbed were dissolved. Such samples are referred to as post-precipitated colloids. The particles were further aged with stirring in these solutions containing organic matter for an additional 20 min, then collected by filtration. Colloids were post-precipitated with gallic acid (Fischer), tannic acid (Aldrich) and the soluble fraction of a peat material (International Humic Substances Society Standard). In further experiments, colloids post-precipitated with tannic acid were once again allowed to react with  $\text{Fe}^{3+}$  ions as follows: approximately 500 mg of TA-coated particles were suspended in a 150 ppm  $\text{FeCl}_3$  solution whose pH had been adjusted to 2 using 1 M HCl. Over a period of 10 min, and with 300 rpm stirring, the pH was raised to 6 using a 0.3 M  $\text{NaHCO}_3$  solution. The particles were aged for a further 20 min and then collected. Samples were prepared for AFM/CFM experiments by placing a freshly cleaved mica substrate on top of a  $0.45 \mu\text{m}$  filter in a filtration apparatus into which the iron hydrolysis suspension was transferred. As the filtrate was removed, the solids settled and collected on the mica. The filtrate removal flow rate was minimized to form a uniform layer of colloids on the mica slides. The solids deposited on the slide were allowed to dry for 24–48 h prior to analysis. As noted above, they were then exposed to aqueous solutions of varying pH during the chemical force titration measurements.

Gallic acid samples were also prepared on freshly cleaved (100) mica substrates. A  $3.5 \times 10^{-4} \text{ M}$  solution of gallic acid (Aldrich, 97%) in acetone was then dropped on the sample surface. The sample was then allowed to dry for approximately 30 s before being placed on a spin-coater at 400 rpm for 1 min. Acetone was used because the solvent evaporation time was short, and it appeared to produce a much more even film of gallic acid on the surface than deposition from aqueous solution. Peat samples were prepared in a similar manner, using a solution of  $2.06 \text{ g l}^{-1}$  of peat in acetone.

### 3. Results

#### 3.1. IR spectroscopy

IR spectra of the unmodified and variously coated colloids used in the CFM experiments are shown in Fig. 1(a and b), along with spectra of the unbound organic precursor compounds for reference. It may be noted in Fig. 1(a) that upon adsorption of either gallic or tannic acid upon the colloid, essentially all of the peaks observed within the ‘fingerprint’ region of the IR spectra are shifted and broadened relative to the pure organic compounds. The peak that appears in the coated samples at  $1365\text{ cm}^{-1}$  has been noted as being indicative of the presence of  $\text{COO}^-$  groups involved in complex formation with the metal oxide surface [18]. The OH-stretching peak of the

benzoate group in gallic acid, seen at  $3489\text{ cm}^{-1}$  in the inset to Fig. 1(a), also disappears upon adsorption onto the colloid. In contrast, Fig. 1(b) shows that when the soluble peat is adsorbed onto the colloid, there is no shift in peak positions. Comparison of peak positions as indicated by the vertical lines in Fig. 1(b) shows that the spectrum of the colloids postprecipitated with soluble peat appears to be essentially a combination of the spectra obtained from the unmodified hydrous iron oxide colloid and pure peat itself.

#### 3.2. AFM images

AFM images of gallic acid on mica were obtained under a variety of conditions. A typical example of an image acquired under ambient conditions appears in Fig. 2(a). The contrast in

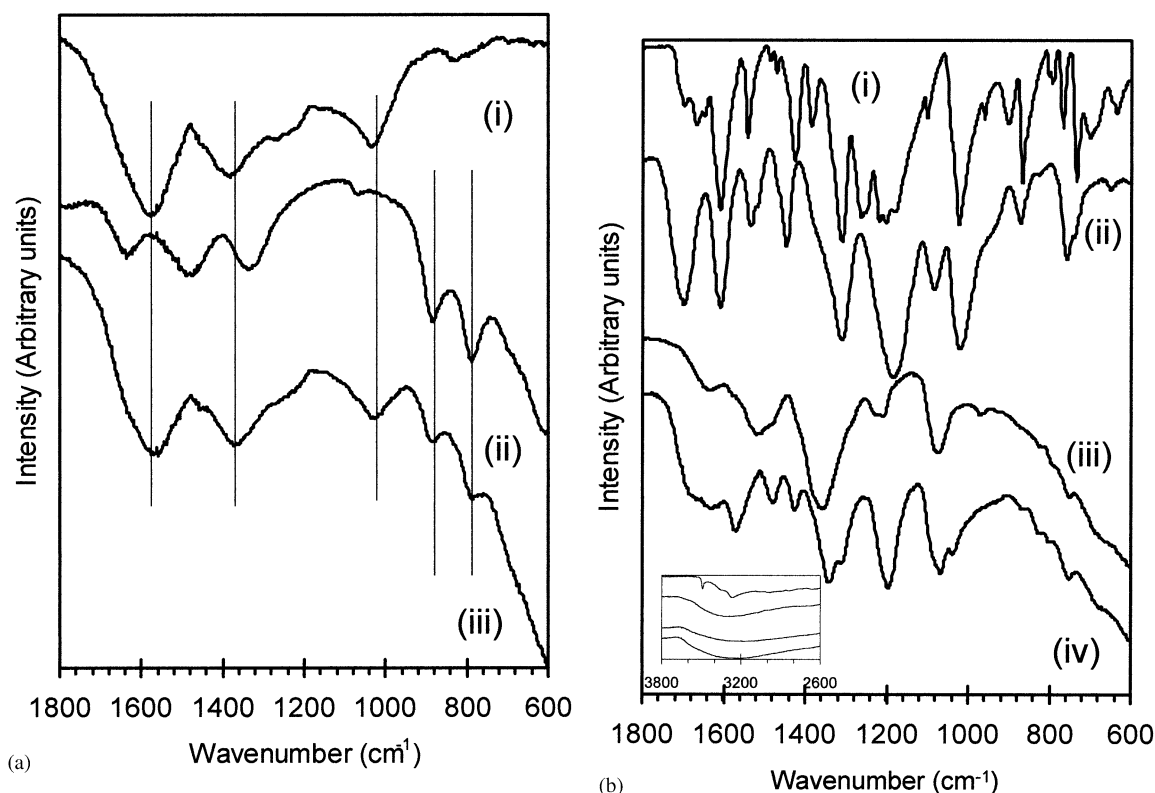


Fig. 1. IR spectra of various colloids and adsorbed organic species. (a) (i) gallic acid; (ii) tannic acid; (iii) a hydrous iron oxide colloid postprecipitated with gallic acid; (iv) the same colloid but postprecipitated with tannic acid. The inset shows the same spectra but in a higher wavenumber region. (b) (i) Peat-derived humic acid; (ii) an unmodified hydrous iron oxide colloid; (iii) the same colloid but postprecipitated with peat-derived humic acid.

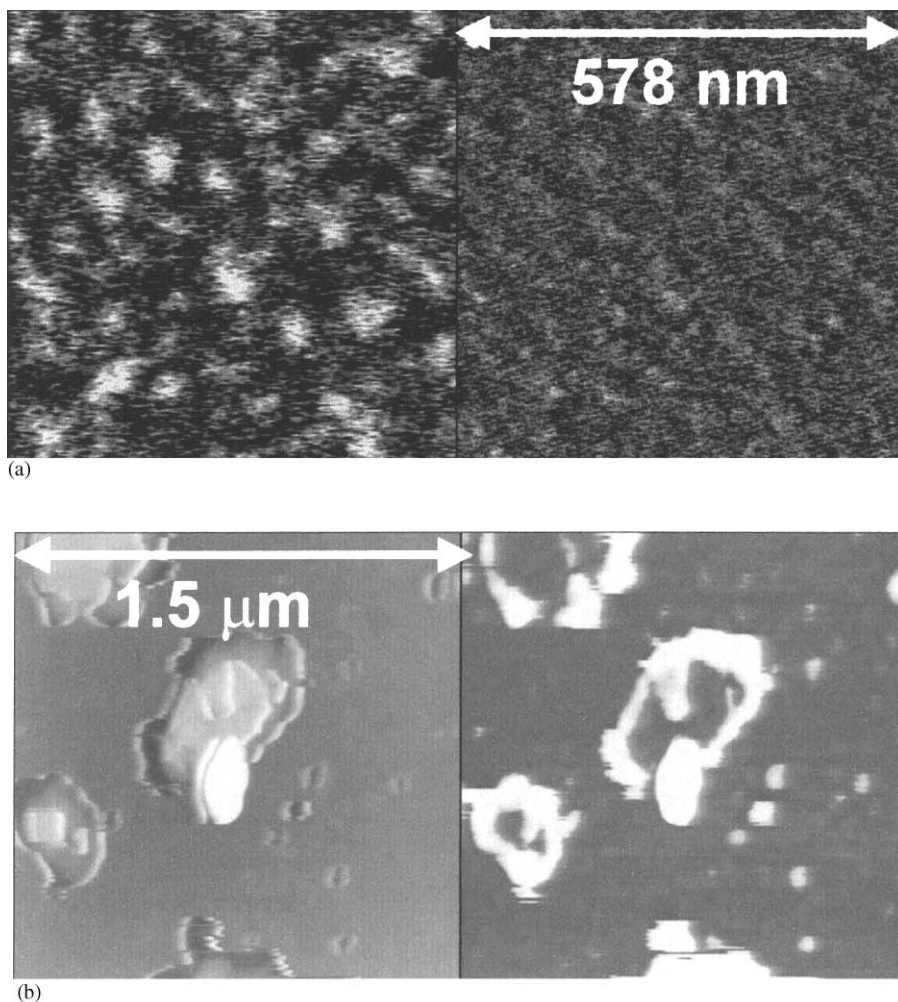


Fig. 2. AFM images of organic acids deposited on mica: (a) gallic acid deposited on the surface. Set point and oscillation amplitude values are 0.75 and 20 nm, respectively. Left hand is in height mode, total  $z$  range of 8.0 nm. Right hand image is the phase shift, total  $z$  range of  $10^\circ$ . All scan dimensions are  $568 \text{ nm}^2$ . (b) Peat-derived humic acid deposited on the surface. Set point and oscillation amplitude are 0.90 and 44 nm, respectively. Left hand image is in height mode, total  $z$  range of 33.9 nm. Right hand image is the phase shift, total range  $13.5^\circ$ . Scan dimensions are  $1.5 \text{ } \mu\text{m}^2$ .

the images was observed to be a strong function of both the set point and tip oscillation amplitude ( $A_0$ ), and contrast changes could be observed at set points below 0.50 and oscillations amplitudes below 20 nm. As can be seen in the images, the gallic acid shows a tendency to form amorphous clumps on the surface. Gallic acid clumps could be imaged on surfaces in solution throughout the pH range of 3.1–9.5.

A similar data set was acquired for the peat on a mica surface, and a typical example is shown in Fig. 2(b). Again, the contrast was a strong function of both the set point and tip oscillation amplitude although no contrast reversals were observed on this sample. The material again remained on the surface in solution under varying pH conditions. Images of the hydrous iron oxide colloid particles themselves were also acquired and

have been published elsewhere [13]. They show a surface that is disordered on a short range scale ( $< 100$  nm) in which the particles are stacked in plate like layers on the mica substrate.

### 3.3. Chemical force titrations

Figs. 3 and 4 show the chemical force titration experiment results for various tip–sample combinations. In all cases, the adhesive force observed is plotted as a function of solution pH. In Fig. 3, the results on a gallic acid coated mica slide are shown. The interaction of the  $-\text{CO}_2\text{H}$ -terminated tip with the gallic acid control surface is shown in Fig. 3, curve (i). Here, a maximum attractive interaction occurs at a pH of 4.5. Fig. 3, curve (ii) shows the results for the same surface, titrated with a  $\text{PO}_2\text{H}$ -terminated tip and reveals a peak at a

pH of 5.3. While the two curves overlap at the high pH end, at lower pH values the  $-\text{PO}_2\text{H}$  curve falls off more rapidly and does not cover so wide a pH range. The control case is shown in Fig. 3, curve (iii) in which a  $-\text{PO}_2\text{H}$ -terminated tip was brought in contact with a freshly-cleaved mica surface. There is relatively little adhesive in this system over the entire pH range measured. Similarly, only a small interaction was observed when titrating a  $\text{CO}_2\text{H}$ -terminated tip on mica.

These results may be compared with those shown in Fig. 4(a) for the  $-\text{CO}_2\text{H}$ -terminated AFM tips titrated against various iron oxyhydroxide colloids deposited on mica slides. Fig. 4(a), curve (i) shows the interaction of the unmodified colloid with the tip. Here, the maximum is broad, and the adhesive interaction remains significant over much of the pH range studied. Using the

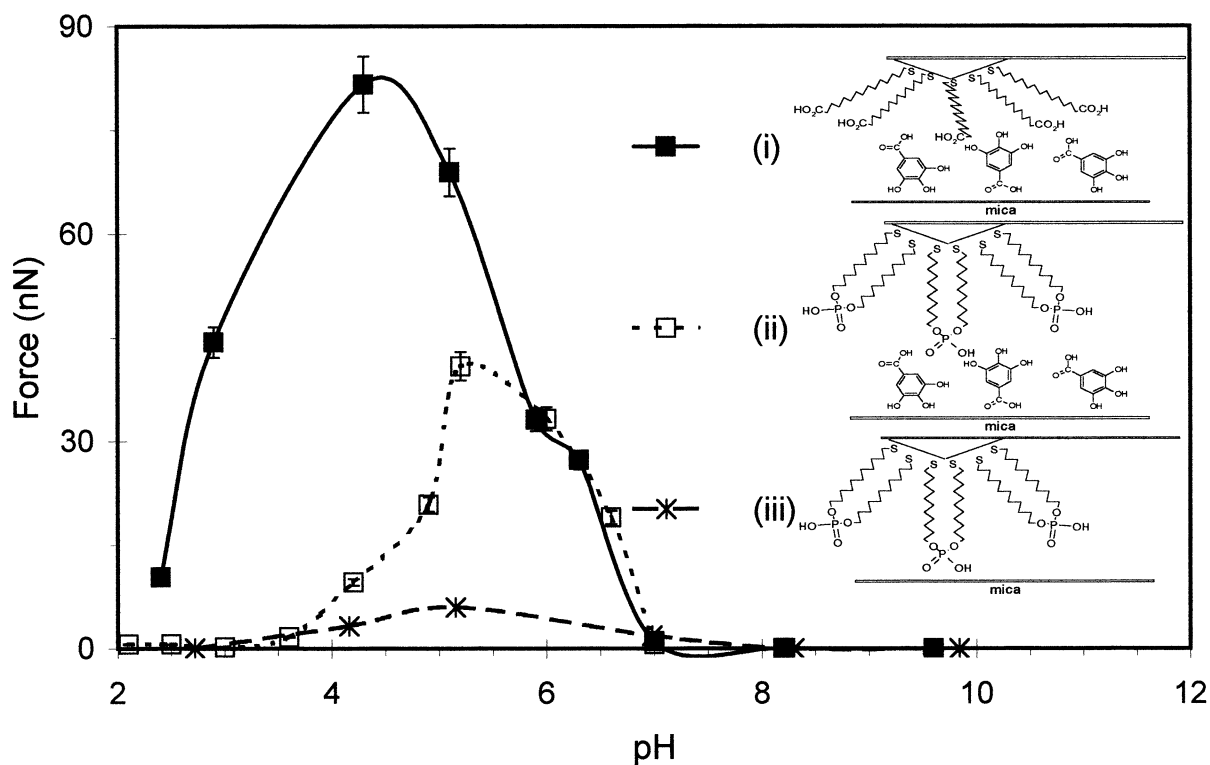


Fig. 3. Chemical force titrations: (i) using a 16-thiohexadecanoic acid terminated tip on tannic acid adsorbed on mica; (ii) using a bis(11-thioundecyl)phosphate terminated tip on tannic acid adsorbed on mica; and (iii) using a bis(11-thioundecyl)phosphate terminated tip on the bare mica substrate. The accompanying figures are meant to schematically represent the various combinations of tip and sample interactions, and (other than the thiol linkage to the surface) are not meant to necessarily represent the actual orientation or density of the molecules on these surfaces.

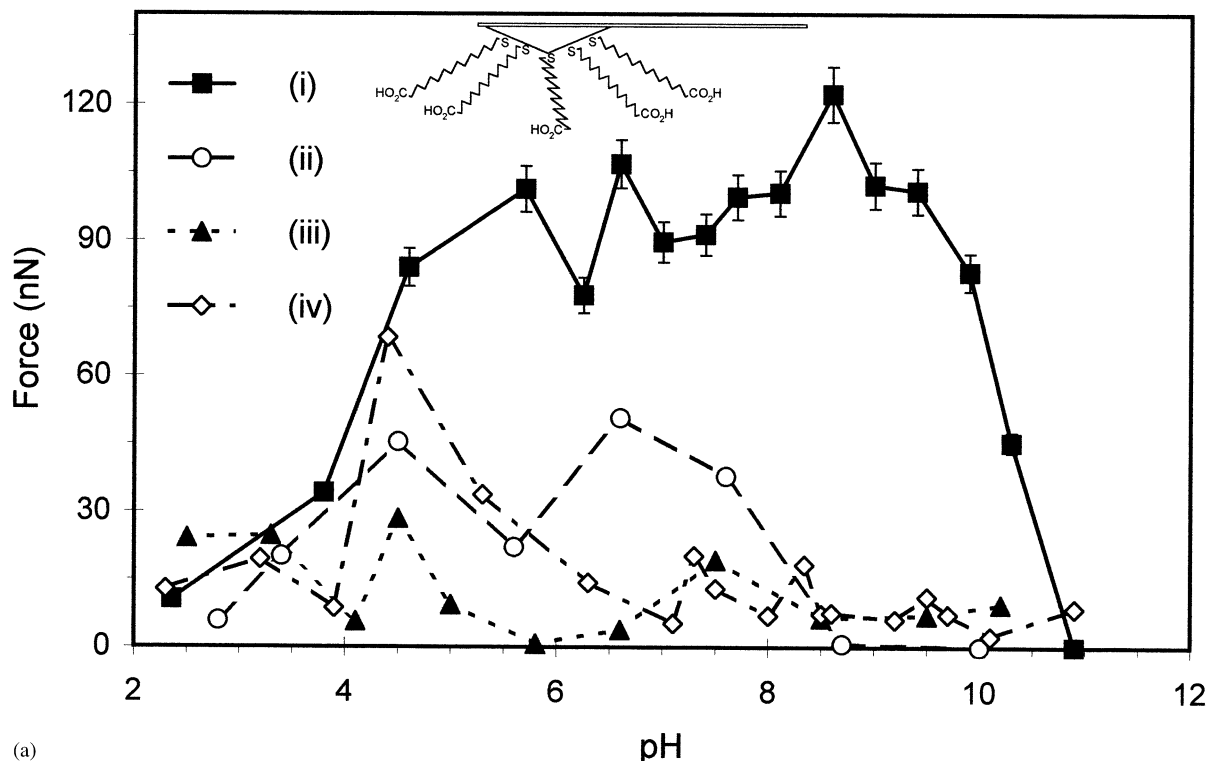


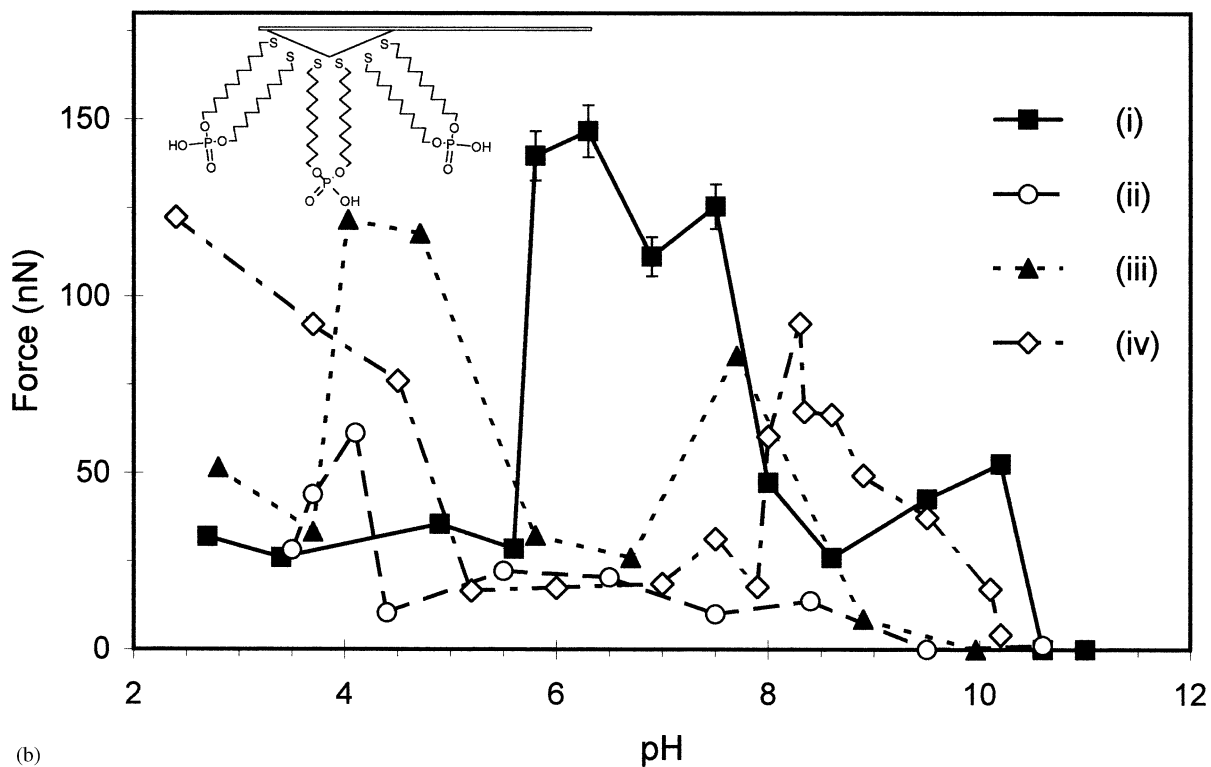
Fig. 4. Chemical force titrations using: (a) a 16-thiohexadecanoic acid terminated tip; and (b) using a bis(11-thioundecyl)phosphate terminated tip (key). The colloids under study are: (i) an unmodified hydrous iron oxide colloid and the same colloid post-precipitated with; (ii) gallic acid; (iii) tannic acid; and (iv) humic acid. The accompanying figures are meant to generally illustrate the various interacting tip and sample combinations, and (other than the thiol linkage to the surface) are not meant to necessarily represent the actual structures or orientations or density of the molecules on these surfaces.

same CO<sub>2</sub>H tip, experiments were carried out with colloids post-precipitated in the presence of; (ii) gallic acid; (iii) tannic acid; and (iv) soluble peat. The overall magnitude of the interaction on these colloids decreased compared to the unmodified colloid, and the pH range over which large adhesive interactions is narrowed and shifted towards lower pH values, especially in the case of the two larger organic acids.

Fig. 4(b) shows the results for a similar set of experiments using a –PO<sub>2</sub>H-terminated tip. On the unmodified colloid, seen in curve (i), a maximum appears over a relatively narrower pH range centered at a pH of 6.5–7. There is, however, weaker interaction at both high (> 8) and low (< 6) pH ranges. When titrated on a colloid post-

precipitated with gallic acid (ii), the maximum is shifted towards a pH of 4, and the overall adhesive interaction is strongly reduced. On the colloid post-precipitated with tannic acid (iii), the maximum adhesive interaction is similarly shifted towards a pH of 4, while with the colloid post-precipitated with soluble peat (iv) the adhesive interaction is shifted to even lower pH values. In these latter two cases, we also see a second peak in the force titration with maximum centered near pH 8.

Fig. 5 shows the results of the –PO<sub>2</sub>H force titration on a sample postprecipitated first with tannic acid and then further exposed to a fresh solution containing FeCl<sub>3</sub> as a source of Fe<sup>3+</sup> ions. Two peaks are again observed: one maximiz-



(b)

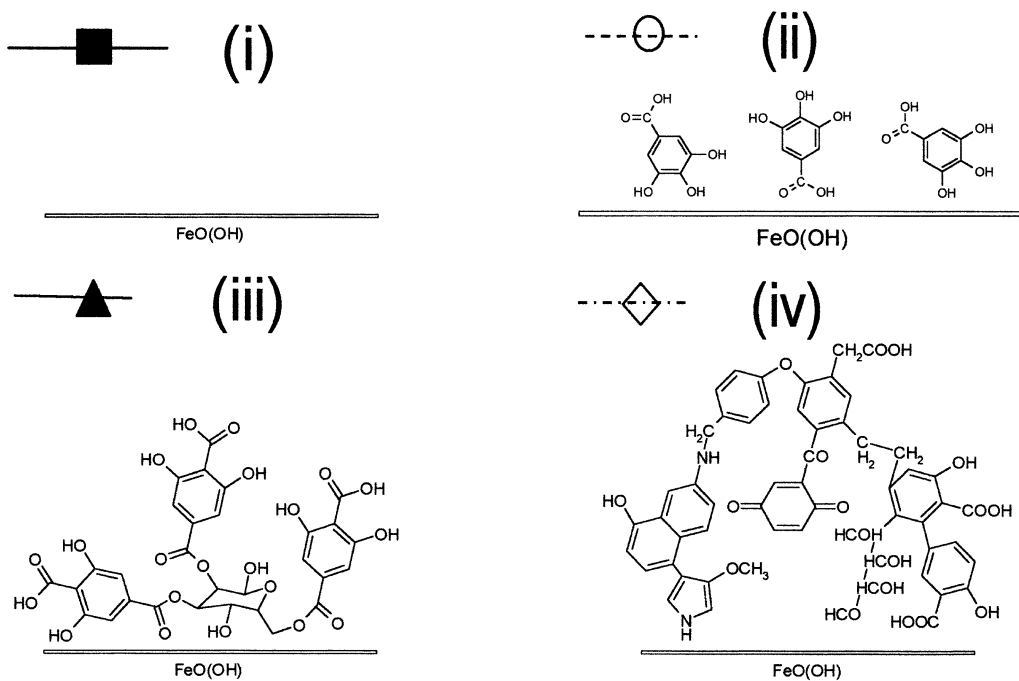


Fig. 4 (Continued)

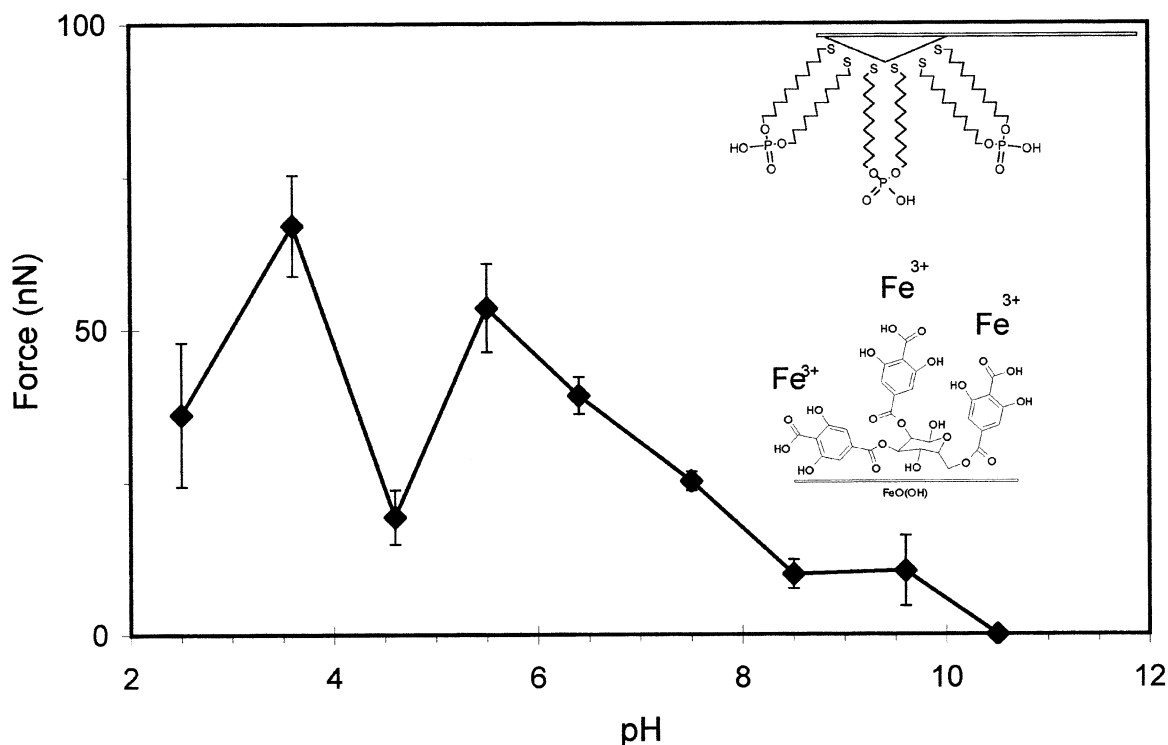


Fig. 5. Chemical force titrations using a bis(11-thioundecyl)phosphate terminated tip on a colloid post-precipitated with tannic acid and subsequently exposed to a 50 ppm solution of  $\text{FeCl}_3$ , allowing the adsorption of  $\text{Fe}^{3+}$  ions into the tannic acid overlayer. The accompanying figure is meant to schematically represent the system under study and is not meant to necessarily represent the actual orientation or density of the molecules on these surfaces.

ing at a pH of 3.5, similar to the result with the colloid postprecipitated with tannic acid, and a second, broad peak centred at a pH of 5.5.

#### 3.4. Zeta potential measurements

As shown in Fig. 6, zeta potential measurements were carried out on the colloidal systems to characterize their surface charge as a function of pH. It can be seen that the point of zero charge (pzc) of the colloids shifts to lower pH values (i.e. the colloid becomes more acidic) as we move from the unmodified colloid at a pH of 5.5 (i) to those post-precipitated with gallic acid at a pH of 4.0 (ii) and tannic acid at a pH of 2.5 (iii). The colloid post-precipitated with soluble peat (iv) at a pH of 3.5, has an isoelectric point closer to that of the gallic acid-coated colloid.

## 4. Discussion

### 4.1. IR spectroscopy

Several peaks in the IR spectrum can be readily assigned: for example, the broad peak at  $1612\text{ cm}^{-1}$  that appears in the spectrum of the unmodified colloid (Fig. 1(b), curve (ii)) which also appears as a shoulder in the modified colloid spectra, can be ascribed to water adsorbed within the colloids. Likewise, the weak transitions at  $870\text{ cm}^{-1}$  and  $775\text{ cm}^{-1}$  in the colloid spectra are probably due to Fe–O vibrational modes. The shifts in IR peak position when gallic or tannic acid were adsorbed on the colloids are difficult to interpret due to the complexity of the spectra, but some general observations may be made. Most importantly, the fact that peaks within the fingerprint

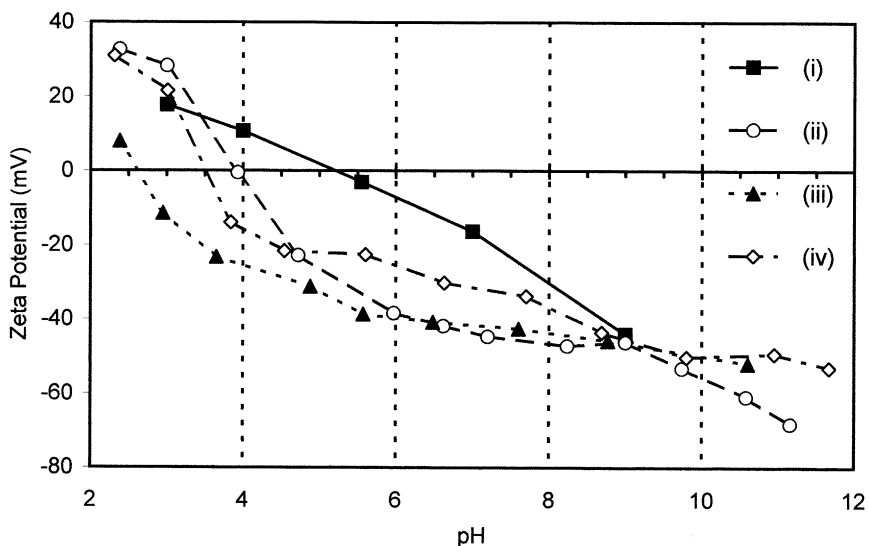


Fig. 6. Zeta potential of various colloids as a function of pH. (i) Unmodified hydrous iron oxide colloid and the same colloid post-precipitated with; (ii) gallic acid; (iii) tannic acid; and (iv) humic acid.

region of the IR spectrum shift upon adsorption show that the gallic and tannic acid have been chemisorbed onto the colloid surface. In the case of the gallic acid, the disappearance of the benzoate OH stretch at  $3489\text{ cm}^{-1}$  demonstrates that the gallic acid is binding to the surface through this group, in agreement with previous workers [6,7]. This is also supported by the appearance of the peak at  $1365\text{ cm}^{-1}$  in the spectra of the colloids on which tannic or gallic acid are adsorbed (curves (iii) and (iv) of Fig. 1(a)). This peak is indicative of binding between  $\text{COO}^-$  groups and the oxide surface. In the case of gallic or tannic acid adsorption, the only peak that does not shift in position is that at  $1303\text{ cm}^{-1}$  in tannic acid (curve (ii) of Fig. 1(a) and appearing as a distinct shoulder in curve (iv) in Fig. 1(a)). This might be due to a phenol stretching mode from a phenol site far from the surface when this bulky molecule is adsorbed on the surface. The lack of any spectral shifts with the peat-derived humic material indicates that this much bulkier species has been physisorbed on the surface or that functional groups giving rise to the spectra are not involved in binding.

#### 4.2. Gallic and humic acid surfaces

Several control surfaces were investigated as part of the CFM experiments, in addition to the colloids themselves. One of these was gallic acid adsorbed on mica. The AFM images in Fig. 2(a) show that gallic acid forms an amorphous layer when a thin layer is spin coated on mica. It is clear that depending on the imaging conditions used, that the contrast and resolution of the images may change quite dramatically. Similar effects of changing set point and oscillation amplitude have been seen in the case of various polymer systems [14–18], on stearic acid monolayers on Au(111) [19] and for aluminum oxide colloids [20]. The humic acid shows similar trends in the image contrast with changes in oscillation amplitude and set point. Like gallic acid, the peat-derived humic material formed amorphous clumps on the surface, although the layer was not nearly so continuous.

We now consider the results of the force titration experiments on gallic acid. Gallic acid contains two types of ionizable sites: the carboxylate group with a  $\text{pK}_a$  of 4.2 and three phenolic

groups, the first of which has a  $pK_a$  of 8.78 [21], with the other  $pK_a$  values above the pH range examined here. The  $pK_a$  of the acid group for a long chain carboxylic acid in solution, such as the 16-thiohexadecanoic acid used on the probe tip, is generally quoted as 4.8. However, previous workers have found that in the case of self-assembled monolayers of  $\text{CO}_2\text{H}$ -terminated thiols, this value is shifted upwards to 5.2, due to the reduced solvation of the end groups on the self-assembled monolayer [22,23]. The titration curve from Fig. 2(i) for the  $\text{CO}_2\text{H}$  terminated tip on gallic acid, with its adhesive maximum near a pH of 4.5 is consistent with a model in which the tip-sample interaction is dominated by H-bonding effects. At or just above a pH of 4.5, both tip and sample should be approximately 50% ionized. Under these conditions, we should expect H-bonding to be maximized between the two, leading to a large attractive force between tip and sample. Below a pH of 4, both tip and sample are fully protonated, and while H-bonding may still take place, it is less effective than in the partially ionized case, with a concomitant decrease in adhesive force. Above a pH of 4, we expect the adhesive interaction to fall off rapidly as both tip and sample are deprotonated and a repulsive interaction arises between the negatively charged surfaces. In fact, the adhesive interaction appears to remain significant to a pH of about 7. This is presumably due to the fact that the phenol sites on the gallic acid, some of which would remain protonated up to pH values in excess of 11, are also available for H-bonding in which the forces are sufficiently large to overcome the repulsive interactions. The one difficulty to account for in this model is the fact that we observed no adhesive interaction in the region of pH 7. However, in these control cases, we should also consider the effect of the mica substrate on the tip-sample interaction. The mica surface is charged in aqueous solution and is known to have a negative potential over the pH range used here, becoming more negative at high pH values [24]. Such a negative charge could overwhelm any attractive interaction between the tip and sample at high pH values.

We have measured a  $pK_a$  of 5.0 for the  $-\text{PO}_2\text{H}$  terminated tip by force titration of a bis(11-

thioundecyl)phosphate tip on a substrate containing a SAM of the same species [13]. In such an experiment, a maximum adhesive interaction is observed, for reasons similar to the arguments above, at the  $pK_a$  of the SAM. Given that the surface  $pK_a$  of the carboxylate and phosphate tips are so similar, we should expect similar behavior as with the  $-\text{CO}_2\text{H}$  tip in the force titration curve, assuming a system dominated by H-bonding effects. Indeed, a maximum is observed in Fig. 2(ii) for the  $-\text{PO}_2\text{H}$ -gallic acid system at a pH of 5.3, followed by a rapid drop off to higher pH that mirrors the  $-\text{CO}_2\text{H}$ -gallic acid case. At higher pH the fall off in adhesive force in both systems must presumably be dominated by electrostatic repulsion between deprotonated and negatively charged tip and sample surfaces.

#### 4.3. Chemical force titrations on the bare colloid

We now consider the behavior of the tips when titrated on the various colloid surfaces. X-ray diffraction analysis of the colloids has demonstrated that they are entirely amorphous. Previous work using AFM imaging [13] has shown that on mica the colloidal iron oxy hydroxide particles deposit into a continuous layer which has regions in which the amorphous particles deposit in plate-like crystallites and others in which the particles are deposited in a more disordered manner. Because of the amorphous nature of the particles we would expect there to be a variety of surface sites available with a series of  $pK_a$  values.

The surfaces of crystalline forms of iron oxides and hydroxides, such as the minerals goethite, hematite or lepidocrocite, are known to have three distinct hydroxyl sites [9,25–28]. These include the A, or oxo site, in which a hydroxyl group is bound to a single iron atom, i.e.  $\text{FeOH}$ . This site is amphoteric, and may exist in  $\text{FeOH}_2^+$  or  $\text{FeO}^-$  forms, depending on pH. The first  $pK_a$  of the A site (i.e. for  $\text{FeOH}_2^+/\text{FeOH}$ ) is reported to lie in the range of 4.2–7.09, depending on the crystal face and species studied. The (second)  $pK_a$  for the A site is believed to lie in the pH 8–10 range. The remaining two sites are basic. These are the C or  $\mu$ -oxo site, where oxygen bridges to two irons,  $\text{Fe}_2\text{O}$  (protonated form  $\text{Fe}_2\text{OH}^+$ ) and the B or  $\mu_3$ -oxo

site, where oxygen is bound to three irons,  $\text{Fe}_3\text{O}$  (protonated form  $\text{Fe}_3\text{OH}^+$ ). The  $\text{p}K_{\text{a}}$  values for deprotonation of the B and C sites have been calculated to lie in the range of 8.05–9.79, again depending on the species and crystal face [25], although some authors have reported values as high as 11 for these sites [27]. For an amorphous system we may consider then that there are generally two pH ranges of consequence: the first around a pH of 6 corresponding the  $\text{p}K_{\text{a}1}$  of the A site, and a second higher pH region around pH 8–10 above the  $\text{p}K_{\text{a}2}$  of the A site and the  $\text{p}K_{\text{a}}$  of the B and C sites.

The calculated surface isoelectric point for goethite is at a pH of about 9 [25]. Isoelectric points for some other minerals, such as hematite are somewhat lower, nearer to a pH of 7. The isoelectric point for the unmodified colloid as measured here using zeta potentials (Fig. 6) is at a pH of 5.5, and the charge on the colloids becomes sharply negative at high pH values. This isoelectric value, of course, is much lower than the theoretical one for goethite but is in fact similar to values obtained by other workers [29]. The isoelectric point of iron hydroxide colloids is highly sensitive to the adsorption of trace ions in solution, particularly  $\text{Cl}^-$  ion or bicarbonate ion arising from dissolved  $\text{CO}_2$  in solution. The adsorption of these ions may decrease the isoelectric point by as much as a pH unit [27,29]. Indeed, upon rinsing our colloids three times with a 0.1 M NaOH solution, the isoelectric point was seen to shift from 5.5 to 6.4, presumably because of removal of residual  $\text{Cl}^-$  ions from the colloid surface.

The modified AFM tips may in principle interact with any of the iron oxide sites on the surface. If we accept a model based on a combination of electrostatic and H-bonding arguments, such as was the case for the tip interactions with the gallic acid surfaces, we might expect to see an adhesive interaction across a broad pH range as is observed with the carboxylic acid tip on the colloid in curve (i) of Fig. 4(a). As the pH is increased above 4, the tip becomes negatively charged, and interacts strongly with positively charged sites on the colloid surface. The B and C sites in particular are only deprotonated at pH values above 8 on the

colloid, and the tip–sample interaction remains significant up to a pH of about 10, at which point both tip and sample have become negatively charged, leading to a rapid decrease in adhesive interaction. The force titration results then are consistent with the carboxylic acid tip interacting with all three binding sites on the surface. The large magnitude and breadth of the pH range of the adhesive forces in this system may be taken to suggest that interactions between the  $\text{CO}_2^-$  groups of the probe SAM and surface  $\text{Fe}^{3+}$  ions can occur at oxo sites in both protonated and neutral forms.

The phosphate tip also shows a large adhesive interaction, however over a much narrower range of pH values relative to the carboxylate tip, between 6 and 8 as seen in Fig. 4(b), curve (i). The fact that the two tips show such different behavior, given that they have similar  $\text{p}K_{\text{a}}$  values, is of itself strong evidence that in the whole of this work we are observing interactions that arise not from some general Debye screening or zeta potential effect, but from chemically specific tip–sample interactions. The phosphate–colloid adhesive interaction is centered at the first  $\text{p}K_{\text{a}}$  of the A site and is consistent with this tip interacting mainly with this site on the surface. In this case, the maximum interaction begins in the pH range at which the tip ( $\text{p}K_{\text{a}}$  of 5) has deprotonated while the surface A site is positively charged. The  $(\text{RO})_2\text{PO}_2^-$  group on the tip can then react with the  $\text{FeOH}_2^-$  surface site. As the pH increases past 8, the A site loses its first proton, and the interaction is no longer as favourable. The plateau regions below pH 6 and above pH 8 show that there is perhaps a minimal interaction with the B and C sites with the tip as well. Our CFM observations are consistent with the findings of previous workers that the A site is the preferred site at which orthophosphate ion adsorbs from solution [30]. Zeta potential and absorption measurements [8] as well as IR spectroscopy [30] have suggested that the phosphate ions form bidentate covalent complexes with adjacent A sites on the surface. The complexes thus formed are known to be highly stable, and the retained phosphate does not readily desorb or exchange with competing ions in solution. Thus, the magnitudes of the force interaction of the phosphate and

carboxylate tip in principle should also differ considerably. In practice, it is difficult to compare the overall magnitude of the interactions between two different tips, due to uncertainties in the tip–sample contact area (i.e. tip radius) and the packing density of the thiol-based chemical probes on the tip surface.

#### 4.4. Chemical force titrations on colloids modified with gallic, tannic and humic acids

Since organic matter is known to block phosphate adsorption on iron colloids, we undertook two other sets of experiments in which colloids post-precipitated with a series of increasingly complex organic compounds—gallic, tannic and humic acids—were titrated against the  $-\text{CO}_2\text{H}$  and  $-\text{PO}_2\text{H}$  tips. Generic chemical structures of tannic and humic acid are shown in Fig. 4. Tannic acids consist of a distribution of gallic and benzoic acid groups attached through ester linkages to a glucose center and are dominated by their peripheral aromatic acid and phenolic functional groups. Humic acid can be more complex, and contains aliphatic substituents in addition to aromatic phenol and acid groups.

As noted above, evidence has been seen that molecules such as gallic acid bind to the surface in a bidentate fashion, via the benzoic acid group and an adjacent phenol group [7]. Such adsorption obviously must have the effect of consuming and thus blocking surface binding sites, and as such, reduction in the interaction of the tip with the surface. As seen in Fig. 4(a), curve (ii), this appears to be the case with the carboxylate tip. The interaction at higher pH values is very significantly reduced, suggesting that the B and C sites especially are being occupied or at least blocked by gallic acid. The shift of the interaction to low pH is also consistent with the zeta potential measurements on the modified colloids which show that they become much more acidic when post-precipitated with the organic acids. In the case of the larger organic acids, the titration curves (iii) and (iv) in Fig. 4(a) show strong interactions only near a pH of 4. This is close to the  $\text{p}K_{\text{a}}$  of both the tip and the benzoic or alkanolic acid groups that are present in tannic and humic acids, demonstrating

that the main interaction in these cases is H-bonding with carboxylic acid groups as was observed with the control gallic acid experiments described earlier. This is particularly apparent with the peat-derived humic material, which has qualitatively a very similar titration curve to that seen for the carboxylate tip on the gallic acid sample shown in Fig. 3. The similarity is not surprising in that soluble humic material is the bulkiest of the three organic sorbates, and would most effectively screen the tip from residual iron oxide surface sites. In the case of the smaller gallic acid, there are still residual interactions at higher pH indicating that not all underlying sites have been completely blocked.

In the low-pH regime the interaction of the phosphate tip with the organic-modified colloids shows similar trends to the interactions with the carboxylate tip. For the gallic-acid coated colloid, the adhesive interaction in Fig. 4(b), curve (ii) shows a small peak at a pH of 4 and a weak interaction region at higher pH values. Presumably far fewer sites remain available for phosphate interactions on the surface. On the colloids post-precipitated with tannic acid or peat-derived humic material, we see the adhesive interaction form two maxima at pH values that are close to those of benzoic acid and phenol. Here, we expect that the large organic compounds will sterically hinder the approach of the tip to the iron oxide surface, and block its interaction with reactive sites, accounting for the drop in adhesive interaction in the mid-pH range (6–7). The phosphate tip then encounters benzoic acid and phenolic groups on the surface (and in the case of humic acid, alkanolic groups as well), leading to the observation of the two new force titration features. We had earlier noted that where the gallic acid was deposited directly on mica, the negative charge of the substrate may have inhibited adhesion forces at high pH. No such inhibition was noted here, where the underlying substrate was the hydrous iron oxide colloid.

#### 4.5. Tannic acid colloids modified with $\text{Fe}^{3+}$

On the basis that organic matter can inhibit phosphate adsorption through the occupation and

blocking of metal oxide surface sites, it is easily imagined that the phosphorus adsorptive ability of a soil inversely correlates with its organic carbon content. This is the case for many soils; however in others, such as Podzolic soils, the reverse effect has been observed. Podzolic soils are known to have iron atoms complexed to humic materials, and bind phosphate through humic- $\text{Fe}^{3+}$ -phosphate bridges [31]. In fact, soils having iron atoms organically complexed to humic substances have been reported to have over eight times the phosphate adsorption capacity of hydrous iron oxide particles [32]. To probe this effect by CFM, a sample of hydrous iron oxide colloids post-precipitated with tannic acid was reacted further with a  $\text{FeCl}_3$  solution. The result of the  $-\text{PO}_2\text{H}$  force titration on this system is shown in Fig. 5. In comparison to the results in Fig. 4(b) (i) and (iii) for the unmodified and tannic acid coated colloids, respectively we may note that the maximum near pH 7 is once again observed in addition to a second peak at pH 4, presumably arising still from the tip interaction with benzoate groups. This observation suggests that the phosphate groups on the  $-\text{PO}_2\text{H}$  CFM probe indeed interact in a fundamentally similar manner with organically complexed  $\text{Fe}^{3+}$  ions as they do with  $\text{Fe}^{3-}$  ions at the hydrous iron oxide surface, consistent with the hypothesis that Podzolic soils adsorb phosphate through bridging humic- $\text{Fe}^{3+}$ -phosphate interactions [33].

## 5. Conclusions

The adhesive interactions between both phosphate and carboxylate-terminated AFM tips and a series of hydrous iron oxide colloids and gallic acid coated surfaces have been examined as a function of pH. AFM imaging of the gallic acid surface demonstrates the presence of both crystalline and amorphous regions on the surface. The gallic acid could be readily distinguished from the mica surface upon which it was deposited by means of tapping mode AFM, due to the different mechanical properties of the two materials.

Chemical force titrations on gallic and tannic acid demonstrated that the main interaction be-

tween either tip and these substances occurred through H-bonding. However, for the interaction of the tips with unmodified colloids, a model of specific adsorption appears to be required. In the case of the phosphate, a specific, strong interaction, presumably via a  $\text{Fe}-\text{O}-\text{P}$  bond at a site equivalent to the A ( $\text{FeOH}$ ) site of goethite was observed. In the case of the carboxylate, the interaction was also strong but less specific, and extended over a much broader pH range, suggesting that the tip was also able to interact at B and C sites.

The adsorption interactions of both carboxylate and phosphate tips with colloids post-precipitated with gallic, tannic or peat-derived humic material, were significantly changed in relation to unmodified colloids. In both cases the organic molecules appeared to block the interaction of the phosphate tip with the iron oxide surface and largely eliminate the strong adsorption interactions that centered around pH 6. Additionally, new force titration features having maxima about pH 4 and 8 appeared for these samples, which were presumably due to H-bonding between the tip and benzoic acid and phenolic groups of the organic acid on the surface. The interaction of the  $-\text{PO}_2\text{H}$  CFM probe surface to which  $\text{Fe}^{3-}$  ions had been post-precipitated onto a previously tannic acid-coated surface gave rise to adhesive interaction with maximum again at about pH 6, i.e. fundamentally similar to that seen for the  $-\text{PO}_2\text{H}$  probe on the unaltered hydrous iron oxide surface. This observation supports the supports a model involving the formation of humic- $\text{Fe}^{3+}$ -phosphate bridges in podzolic soils.

## Acknowledgements

We acknowledge the Natural Sciences and Engineering Research Council of Canada for financial support. Dr H.F. Shurvell is acknowledged for assistance with IR measurements.

## References

- [1] C. Lui, P.M. Huang, *Can. J. Soil Sci.* 80 (2000) 445.

- [2] F.M.M. Morel, P.M. Gschwend, in: W. Stumm (Ed.), *Aquatic Surface Chemistry*, John Wiley and Sons, New York, 1991, p. 508.
- [3] D. Lopez-Hernandez, G. Siegert, J.V. Rodriguez, *Soil Sci. Soc. Am. J.* 50 (1986) 1460.
- [4] F. Liu, J. He, C. Colombo, A. Violante, *Soil Sci.* 164 (1999) 180.
- [5] K. Hunter, P.D. Carpenter, D. Hawke, *Environ. Sci. Technol.* 23 (1989) 187.
- [6] M.I. Tejedor-Tejedor, E.C. Yost, M.A. Anderson, *Langmuir* 6 (1990) 979.
- [7] M.I. Tejedor-Tejedor, E.C. Yost, M.A. Anderson, *Langmuir* 8 (1992) 525.
- [8] L. Li, R. Stanforth, *J. Colloid Interface Sci.* 230 (2000) 12.
- [9] C.R. Evanko, D.A. Dzombak, *Environ. Sci. Technol.* 32 (1998) 2846.
- [10] J.C. Crittenden, S. Sanonraj, J.L. Bulloch, D.W. Hand, T.N. Rogers, T.F. Speth, M. Ulmer, *Environ. Sci. Technol.* 33 (1999) 2926.
- [11] M.G. Nooney, T.S. Murrell, J.S. Corneille, E.I. Rusert, L.R. Hossner, D.W. Goodman, *J. Vac. Sci. Technol. A* 14 (1996) 1357.
- [12] C.M. Eggleston, S.R. Higgins, P.A. Maurice, *Environ. Sci. Technol.* 32 (1998) 456.
- [13] D.I. Kreller, G. Gibson, G.W. vanLoon, J.H. Horton, *J. Colloid Interface Sci.* in press (2002).
- [14] M. Verzele, P. Delahaye, C. Dewaele, *Bull. Soc. Chim. Belg.* 93 (1984) 151.
- [15] W. Han, S.M. Lindsay, T. Jing, *Appl. Phys. Lett.* 69 (1996) 4111.
- [16] N. Nakashima, T. Taguchi, *Colloid Surf. A* 103 (1995) 159.
- [17] J.L. Hutter, J. Bechhoefer, *Rev. Sci. Instrum.* 64 (1993) 1868.
- [18] A. Violante, P.M. Huang, *Soil Sci. Soc. Am. J.* 48 (1984) 1193.
- [19] M.O. Finot, M.T. McDermott, *J. Am. Chem. Soc.* 119 (1997) 8564.
- [20] A. Omoike, G. Chen, G.W. van Loon, J.H. Horton, *Langmuir* 14 (1998) 4731.
- [21] I. Boyd, E.G. Beveridge, *Microbios* 24 (1979) 173.
- [22] E.W. van der Vegte, G. Hadziioannou, *J. Phys. Chem. B* 101 (1997) 9563.
- [23] D.A. Smith, M.L. Wallwork, J. Zhang, J. Kirkham, C. Robinson, A. Marsh, M. Wong, *J. Phys. Chem. B* 104 (2000) 8862.
- [24] P. Kekicheff, S. Marcelija, T.J. Senden, V.E. Shubin, *J. Chem. Phys.* 99 (1993) 6098.
- [25] A.R. Felmy, J.R. Rustad, *Geochim. Cosmochim. Acta* 62 (1998) 25.
- [26] J.D. Russell, R.L. Parfitt, A.R. Fraser, V.C. Farmer, *Nature* 248 (1974) 220.
- [27] R.M. Cornell, U. Schwertmann, *The Iron Oxides: Structure, Properties, Occurrences and Uses*, VCH, Weinhamm, 1996, p. 222.
- [28] A. Gualtieri, P. Venturelli, *Am. Mineralogist* 84 (1999) 895.
- [29] P. Heseleitner, D. Babic, N. Kallay, E. Matijevic, *Langmuir* 3 (1987) 815.
- [30] P. Persson, N. Nilsson, S. Sjöberg, *J. Colloid Interface Sci.* 177 (1996) 263.
- [31] C.C. Weir, R.J. Soper, *Can. J. Soil Sci.* 43 (1963) 393.
- [32] J. Gerke, R.Z. Hermann, *Pflanzenernähr. Bodenk.* 155 (1992) 233.
- [33] M. Levesque, M. Schnitzer, *Soil Sci.* 103 (1967) 183.